Characterization of surface films that develop on pre-oxidized copper in anoxic simulated groundwater with sulphide

Colloids and Surfaces A: Physicochemical and Engineering Aspects 676 (2023) 132214

Contents lists available at ScienceDirect

Colloids and Surfaces A: Physicochemical and Engineering Aspects

journal homepage: www.elsevier.com/locate/colsurfa

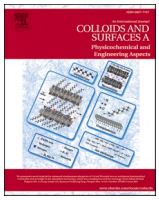

Characterization of surface films that develop on pre-oxidized copper in anoxic simulated groundwater with sulphide

V. Ratia-Hanby [a], E. Isotahdon [a], X. Yue [b], P. Malmberg [c], C. Leygraf [b], J. Pan [b], E. Huttunen-Saarivirta [a,*]

[a] VTT Technical Research Centre of Finland Ltd, Espoo, Finland
[b] Division of Surface and Corrosion Science, Department of Chemistry, KTH Royal Institute of Technology, Stockholm, Sweden
[c] Department of Chemistry and Chemical Engineering, Chalmers University of Technology, Gothenburg, Sweden

GRAPHICAL ABSTRACT

Sulphide content in the groundwater significantly influences the morphology, composition and thickness of the surface film.
The build-up of Cu_2S was evidenced at the sulphide contents of 32 mg/L and 320 mg/L.
GDOES depth profiling (Figure below) revealed that sulphur and oxygen coexisted in the film all through its thickness at the sulphide content of 32 mg/L.
Figure: Elemental depth profiles of oxygen, sulphur and copper for pre-oxidized specimen exposed to simulated groundwater with 32 mg/L sulphide addition.

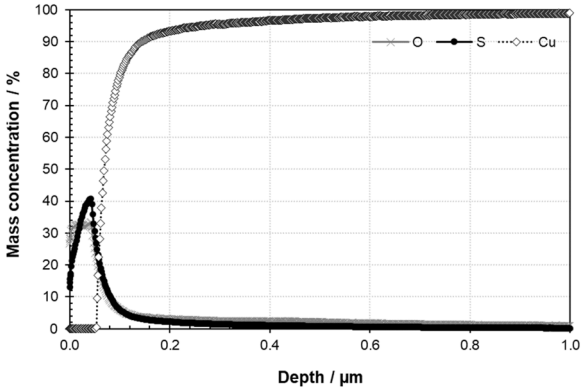

ARTICLE INFO

Keywords:
Copper
Surface film
Copper sulphide
Cuprous oxide
Thickness

ABSTRACT

Surface films formed on pre-oxidized copper in anoxic simulated groundwater with sulphide were characterized by field emission gun scanning electron microscopy (FEG-SEM), Fourier transform infrared spectroscopy (FT-IR), open circuit potential (OCP) measurements, and via analysing the water chemistry and weight changes in the specimens. Additionally, films developed under identical conditions on pre-oxidized and ground copper specimens were characterized by glow discharge optical emission spectroscopy (GDOES). The results revealed that the sulphide content in the groundwater significantly influences the morphology, composition and thickness of the surface film. The build-up of Cu_2S was evidenced at the sulphide contents of 32 mg/L and 320 mg/L. GDOES depth profiling revealed that sulphur and oxygen coexisted in the film all through its thickness, yet the surface

* Corresponding author.
E-mail address: elina.huttunen-saarivirta@vtt.fi (E. Huttunen-Saarivirta).

https://doi.org/10.1016/j.colsurfa.2023.132214
Received 7 June 2023; Received in revised form 30 July 2023; Accepted 8 August 2023
Available online 10 August 2023

was essentially rich in sulphur. The results from characterization are presented in detail in this paper and discussed from the perspective of capabilities of the used methods.

1. Introduction

The final disposal concept for spent nuclear fuel of Finland and Sweden relies on the multi-barrier system with both engineered and natural sealing barriers. The spent nuclear fuel will be first assembled in cast iron containers that are further placed and sealed in copper canisters. The copper canisters will then be positioned in holes drilled into deep bedrock, in the depth of 400–1000 m. Finally, the holes will be filled with bentonite clay, which will swell once in contact with groundwater, being thus compacted, and form a buffer around the copper canisters. [1,2]. Bentonite buffer is believed to provide a favorable environment, in which the integrity of copper canisters should be retained for at least 100,000 years and, in the case of the possible failure, the release of any radioactive nuclides will be held. Hence, in the concept, copper will be the outermost engineering barrier of nuclear waste and the external interface towards the biotic environment of natural barriers.

After several decades of research activities, oxygen-free phosphorus-containing copper (OFP-Cu) has been chosen for the canister material due to its high overall corrosion resistance in anoxic groundwater and sufficient mechanical strength to resist the mechanical loads possibly directed to the canister [3]. In early stages of the final disposal of nuclear waste, oxygen (O_2) exists in the repository, but it is gradually consumed by oxidation reactions. During the oxic period, a film of Cu_2O is known to develop on the copper surfaces in groundwater [4]. Once all oxygen is consumed, the major threat to the long-term durability of the canister is corrosion by sulphur species, in particular sulphide (H_2S, HS^-, S^{2-}) from the dissolution of sulphur-containing minerals in the host rock of the repository, that of pyrite in the bentonite, or from the action of sulphate-reducing bacteria (SRBs) [3].

Plenty of research effort has been put on understanding the corrosion behaviour of copper in the presence of sulphide, e.g., [5–11]. However, in reality, it is the oxidized copper surface that is ultimately exposed to the sulphide-containing environment, not a fresh metal. Smith et al. [12] are among few that have conducted experiments using electrochemically pre-oxidized copper, with the conclusion that the full conversion of a Cu_2O film on copper to Cu_2S in aqueous sulphide solutions occurs chemically at the oxide/solution interface. The conclusion was based on characterization by electrochemical measurements, in-situ Raman spectroscopy and scanning electron microscopy. Forsström et al. [13] have conducted stress corrosion cracking experiments using pre-oxidized specimens and, similarly, documented a full conversion of Cu_2O to Cu_2S upon exposure of OFP-Cu to sulphide- and chloride-containing deoxygenated water at 90 °C. However, a theoretical analysis of interfaces between copper and its oxide and sulphide films [14] provides slightly contradictory view on the topic. By analysing the geometrical match of the interfaces between copper and Cu_2O, and between copper and Cu_2S, Stenlid et al. [14] showed that the structural mismatch values were much larger for the latter pair. It was also demonstrated that low-mismatch facets exist between Cu_2O and Cu_2S, indicating that Cu_2O may act as a bridge between metallic copper and Cu_2S. Additionally, the energetic analyses suggested strong interactions between Cu_2O and Cu_2S but not between metallic copper and Cu_2S, further supporting the multi-layer film development with an Cu_2O inner layer and Cu_2S outer layer. Therefore, the computational approach indicates that the films that develop in sulphide containing environments on pre-oxidized copper are significantly influenced by the nature and structure of the oxide film, which will be retained at Cu-Cu_2S interface as a bridging layer. The experimental results by Hollmark et al. [15] are in agreement with the findings by Stenlid et al. [14] in that when a pre-oxidized copper is subjected to a sulphide containing solution, the resulting film is an admixture of Cu_2O and Cu_2S.

This research is motivated by the aim to shed light in the role of the pre-existing oxide layer on copper in the development of the sulphide film. Our recent work [16] already demonstrated that in the pre-oxidized surfaces exposed to simulated O_2-free groundwater, oxygen and sulphur often coexist. In fact, the results showed that a sulphur-rich inner layer existed between the oxygen-rich outer layer and the copper substrate, indicating that the oxide film does not act as an effective barrier to the sulphide-induced corrosion. This research will, by comparing the surface films that develop in anoxic simulated groundwater at various sulphide concentrations, and the films that form under identical conditions on pre-oxidized and freshly ground copper specimens, provide improved understanding on the structure and chemistry of the films.

2. Experimental

2.1. Exposure of specimens to simulated groundwater

Hot-rolled oxygen-free phosphorus-containing copper (OFP-Cu) provided by Posiva Oyj, Finland, was used as the test material. Specimens of the size of 10 mm × 10 mm x 3 mm were used in the exposures and characterized in-situ and ex-situ. Majority of the exposures were conducted for pre-oxidised copper specimens, which were first wet-ground to 600 grit surface finish (electrochemical and weight loss measurements) or further polished down to 1 μm (microstructural characterization), washed with acetone and ethanol and dried, and then oxidized at the temperature of 90 °C in air for seven days, in order to reproduce the contribution by the oxic period. For comparison, some of the exposures were carried out using copper specimens which were only subjected to wet-grinding to 600 grit surface finish and possibly polished down to 1 μm, washed with acetone and ethanol, and dried, but not subjected to oxidation. All specimens were weighed before and after the experiments, to the precision of 0.0001 g.

The exposure of specimens to simulated groundwater with the addition of selected chemical species was conducted under anoxic conditions. The composition of simulated groundwater is given in Table 1; it has been brought about by modelling the equilibrium chemistry of groundwater at the planned disposal site experiencing ion exchange reactions with the bentonite [17]. A reference exposure was performed using the simulated groundwater as such, yet most of the exposures involved simulated groundwater supplemented with different levels of sulphide (S^{2-}) in the range from $1{\cdot}10^{-4}$ to $1{\cdot}10^{-2}$ mol/L, Table 2. The sulphide additions to the simulated groundwater were made in the form of Na_2S. Before and after the experiments, water chemistry was analysed using standard methods.

Gas-tight glass bottles of the volume of 2 L (specimens for electrochemical measurements) and 5 L (specimens for surface characterization) were used as test vessels. Both the water and the vessels were flushed with argon before the start of the exposure. Vessels were sealed with butyl rubber stoppers to prevent oxygen contamination during the experiment. Further, vessels with electrochemical measurement setup were purged regularly with argon during the exposure period to maintain the anoxic conditions. All exposures were conducted at room temperature (22 °C) for 9 months.

2.2. Characterization of surface films

Characterization of the surface films was done in-situ and ex-situ, yet emphasis was put on the latter. In-situ characterization included electrochemical measurements, which were only done on the selected

specimens. For these specimens, open circuit potential (OCP) and redox potential data were collected continuously throughout the exposure period. OCP measurements employed the copper specimen as a working electrode (WE) and an Ag/AgCl (anaerobic, 0.15 M KCl) as a reference electrode (RE), whereas the redox measurements were conducted against a platinum electrode. Additionally, linear polarization resistance (LPR) and Tafel measurements were conducted once a week with the copper specimen as a WE, another similar copper specimen as a pseudo-RE, and platinum as a counter electrode. LPR measurements were carried over the potential range of ± 20 mV vs OCP, while the Tafel scans were run over the potential range of ± 20 mV vs OCP; both measurements were performed over such a narrow potential range in order to avoid perturbation of the system. Both polarizations were performed at the scan rate of 0.167 mV/s. The electrochemical measurements were performed using a Reference 600™ potentiostat by Gamry Instruments and analysed using a Gamry Echem software. The analysis enables to determine the Tafel constants (β_a, β_c) based on the data from Tafel measurements. Polarisation resistance, R_p, is inversely proportional to the corrosion current I_{corr} as follows [18]:

$$R_p = \frac{B}{I_{corr}} \quad (1)$$

where B is the proportionality constant obtained by:

$$B = \frac{\beta_a \beta_c}{2.3(\beta_a + \beta_c)} \quad (2)$$

Finally, the corrosion rate (CR) was calculated according to:

$$CR = \frac{I_{corr} \bullet K \bullet W_E}{\rho} \quad (3)$$

where K is a constant [which depends on the targeted CR unit; for the unit of mm/a, K is 3272 mm/(A·cm·a)], A is the exposed surface area, a stands for year, W_E is the equivalent weight and ρ the density of copper.

Ex-situ characterization involved the following microstructural characterization methods: field emission gun scanning electron microscopy (FEG-SEM), Fourier-transform infra-red spectroscopy (FT-IR) and Glow Discharge Optical Emission Spectrometry (GDOES). FEG-SEM/EDS investigations were used to provide insights into the morphology of the developed surface films and examine the main elements in the films (acknowledging the poor depth resolution at small film thicknesses). Zeiss UltraPlus Gemini and Zeiss UltraPlus Merlin FEG-SEMs were employed. FT-IR measurements were done using a i-series FT-IR microscope and the related Spectrum BX system by Perkin Elmer, enabling data collection in the wavenumber range from 4000 cm^{-1} to 600 cm^{-1}. GDOES studies were conducted on selected specimens as depth profile analyses of sulphur and oxygen using a GDA 750 HR instrument. The instrument employed the anode of 2.5 mm in diameter.

Additionally, after characterization, removal of the corrosion products was done for some of the specimens to define the related weight change, following ASTM G1–03. Corrosion products were removed chemically, by treating the specimens 3–5 times in a solution containing 500 mL of HCl (37%), 500 mL distilled water and 3.5 g of hexamethylene tetramine ($(CH_2)_6N_4$), i.e., until a steady weight was achieved for the specimen. The solution recipe was adopted from ref. [19].

Table 2
Test matrix in the exposures.

Sulphide (S^{2-}) addition, mg/L	Sulphide concentration, mol/L	Copper surface finish	Methods
0	0	Pre-oxidized	SEM, FT-IR
3.2	$1{\cdot}10^{-4}$	Pre-oxidized	SEM, FT-IR, OCP, redox, LPR, Tafel
32	$1{\cdot}10^{-3}$	Pre-oxidized	SEM, FT-IR, OCP, redox, LPR, Tafel, GDOES
		Ground	SEM, FT-IR, GDOES
320	$1{\cdot}10^{-2}$	Pre-oxidized	SEM, FT-IR

3. Results

3.1. Pre-oxidized specimens

FEG-SEM examinations were conducted for copper specimens before and after pre-oxidation, in order to reveal the morphology of the oxide film, since this was the initial condition of the specimens that were subjected to the test environments. The main observations were that the surface contained shallow grinding grooves from the specimen preparation and the film that was developed during the pre-oxidation process was very thin and covered the entire surface. Additionally, the edges of the grinding grooves occasionally featured preferential oxidation, yet no clear nodule formation was evidenced (Fig. 1). Although not a surface sensitive method, EDS measurements confirmed the presence of traces of oxygen on the surfaces. Example EDS analyses before and after pre-oxidation were 0 wt% (after grinding and before pre-oxidation) and 0.6 wt% (after pre-oxidation).

It is known that FT-IR spectroscopy is a powerful tool in characterizing the oxides on copper [20,21]. Therefore, FT-IR measurements were conducted for the pre-oxidized copper specimens to characterize the nature of the oxide film. The spectrum (Fig. 2) clearly showed the presence of cupric oxide, Cu_2O, via a broad peak starting at the wavenumber of 628 cm^{-1} and extending up to 912 cm^{-1}, with a small shoulder being detected at 826 cm^{-1}. Earlier, the reflection band at the wavenumbers of 620–640 cm^{-1} [20–22] has been assigned to Cu(I)-O vibration mode, thus to Cu_2O, while the broadness of the peak may be explained by the dominant vibrations of copper hydroxyl groups, Cu–O–H, in the wavenumber range of 845 cm^{-1} and 900 cm^{-1} [23]. The remaining bands were related to the chemi- and/or physisorbed molecules of H_2O, CO_2, and O_2 on the surfaces, originating from air. Justin Paul et al. [23] have related the absorption bands between 1100 and 2000 cm^{-1} to the chemi- and/or physisorbed molecules of H_2O and CO_2 on the surfaces, similarly to the double-peak at 2330 and 2350 cm^{-1} (2345 and 2358 cm^{-1}) and peaks at wavenumbers higher than 3000 cm^{-1}, the findings which are further supported by e.g., [24–26]. In particular, it has been reported that the band at 1627 cm^{-1} is due to the H-O-H bending mode, while that at 3429 cm^{-1} corresponds to the vibration mode of −OH group, both indicating the presence of water on the specimen surfaces [27]. The band detected at 1440 cm^{-1} is known to originate from oxygen chemisorbed on the surfaces [28]. The peak at 2920 cm^{-1} is related to C-H vibration mode, i.e., the presence of organic compound, likely acetone [29].

Films formed on pre-oxidized specimens during the exposure to simulated groundwater.

FEG-SEM images, Fig. 3, revealed that surface films developed on the

Table 1
Chemistry of the simulated groundwater adopted from ref. [17]. The ionic species are given in mg/L. Na^+ concentration represents the concentration before the addition of Na_2S.

pH	Cl^-	Na^+	SO_4^{2-}	Ca^{2+}	Mg^{2+}	K^+	Br^-	HCO_3^-	Sr^{2+}	Si^{4+}	B^{2+}	F^-	$C_3H_5O_3^-$
7.8	5274	3180	595	280	100	55	42	14	9	3	1	1	1

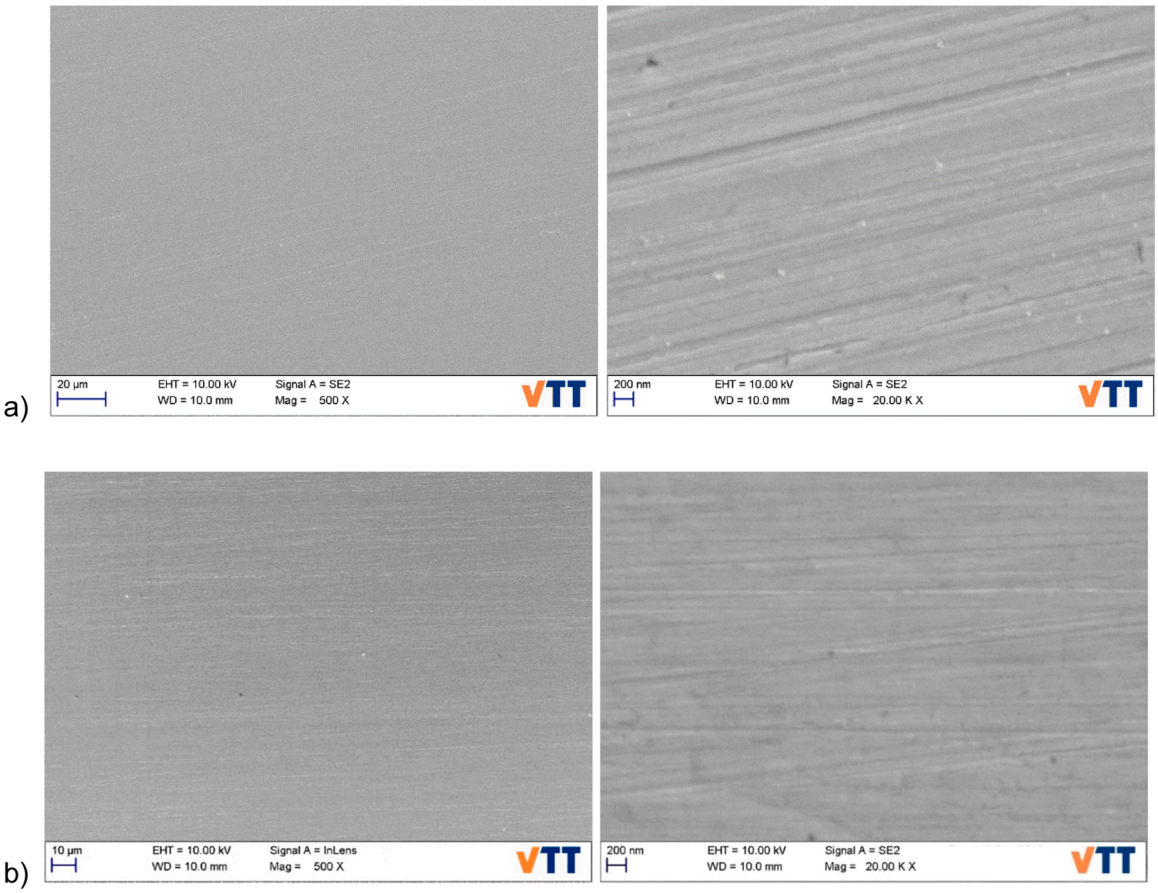

Fig. 1. SEM images, showing the morphology of ground and pre-oxidized OFP-Cu specimens. a) Ground specimens. b) Pre-oxidized specimens.

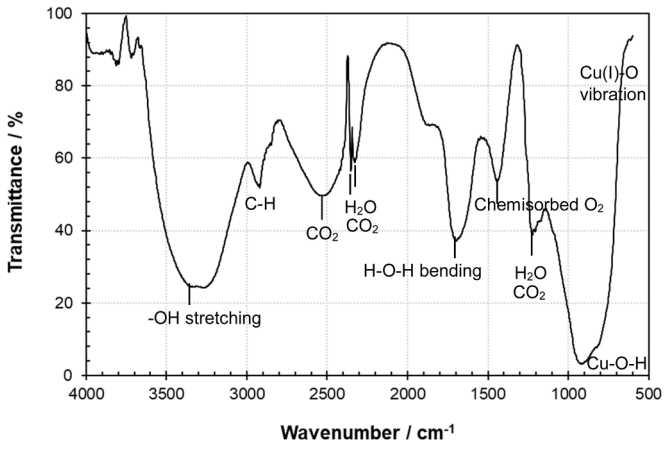

Fig. 2. FT-IR spectrum for the pre-oxidized OFP-Cu specimen.

specimens were continuous and covered all exposed areas. In the absence of sulphide in the test environment, the surface film on the specimens was thin enough to reveal the preferential film growth on grains in a favourable orientation. Nevertheless, nodular film growth was evidenced on top of the continuous thin section (Fig. 3a). At the sulphide content of 3.2 mg/L, the film still followed the morphology of copper substrate, as the grinding grooves were still observable in the specimen surface by SEM. The nodular film growth was even more distinguished than in the absence of sulphide, with the diameter of nodules being up to 1 µm (Fig. 3b). With further increase in sulphide content of the groundwater to 32 mg/L, a change in the film morphology was observed: the film was more uniform than in the previous two cases, with the extent of nodular growth being significantly decreased. Occasional nodules were still detected on the surfaces, but their diameter was typically in the length scale of some hundreds of nanometers (Fig. 3c). At the highest sulphide content (320 mg/L), the frequency of nodules on top of the film was again higher, yet the size of the nodules was not changed (Fig. 3d). In the case of test environment in the absence of sulphides, EDS analyses revealed the presence of minor amounts of oxygen besides copper on the specimen surfaces. In the test environments with sulphide, sulphur and minor amounts of oxygen were detected by EDS analyses on the surfaces in addition to copper. Towards the highest sulphide content, also some magnesium and/or calcium were occasionally detected on the surfaces, likely from the groundwater.

In order to obtain insights into the composition of surface films, FT-IR spectra were collected for the specimens. FT-IR spectra for the pre-oxidized specimens, which were exposed to simulated groundwater with various levels of sulphide additions, are shown in Fig. 4. The spectra revealed clear differences in the composition between the films formed at the sulphide addition of 3.2 mg/L and 32 mg/L, with the former being similar to the spectrum for the film formed without additional sulphide and the latter to that evolved at the highest sulphide content, 320 mg/L. Without additional sulphide and at the lowest sulphide addition, 3.2 mg/L, FT-IR spectra for the specimens contained bands arising from Cu_2O and air-contained molecules, in particular H_2O and CO_2. According to literature, the peaks at the positions of 620–640 cm^{-1}, 790 cm^{-1} 1110 cm^{-1} and 1399 cm^{-1} can be assigned to Cu_2O [30,31], therefore the lowest-wavenumber bands were systematically related to the presence of Cu_2O on the surfaces. As above in the case of pre-oxidized surfaces, many of the bands in the wavenumber range from 1100 and 2000 cm^{-1} and above 3000 cm^{-1} were related to the H_2O and CO_2. For the surfaces exposed to groundwater with the two

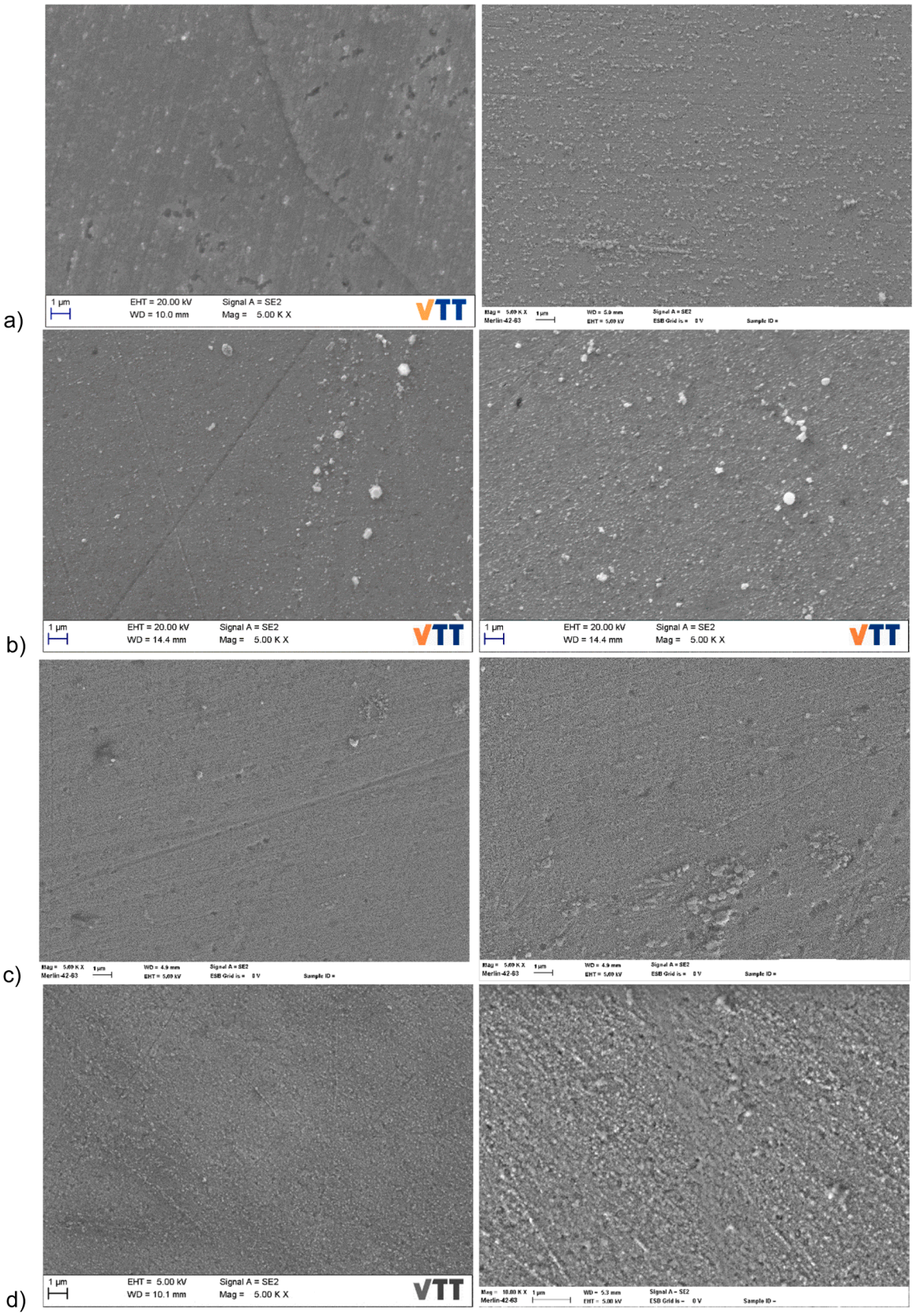

Fig. 3. SEM images of the surfaces after exposure to simulated groundwater with various sulphide amounts: a) 0 mg/L. b) 3.2 mg/L. c) 32 mg/L. d) 320 mg/L. The images on left and right are taken from different areas, therefore they provide complementary view on the morphology.

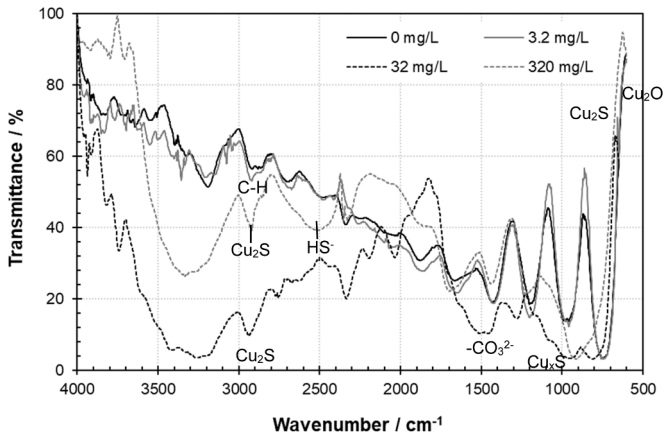

Fig. 4. FT-IR spectra for the pre-oxidized specimens subjected to simulated groundwater with various sulphide additions (0 mg/L indicates the reference simulated groundwater).

highest sulphide contents, FT-IR spectra clearly revealed the presence of Cu_2S. Indeed, the intensity of the lowest wavenumber bands, 650 cm^{-1} and 868 cm^{-1}, was significantly higher in comparison to previous two cases, being related to Cu_2S [32,33] and Cu_xS [34], respectively. Similarly, the band at 2924 cm^{-1}, also linked with the Cu_2S, was particularly pronounced as compared to exposures to simulated groundwaters with lower sulphide contents (0 mg/L, 3.2 mg/L). Additionally, in the case of the sulphide content of 32 mg/L, the adsorption band at the wavenumber of 2500 cm^{-1} was detected, being related to adsorbed HS^- [35], further supporting the contribution of HS^- to the development of the surface film, i.e., Cu_2S. In the case of the sulphide content of 320 mg/L, a strong adsorption band was observed at 1440 cm^{-1}, essentially because of the presence of CO_3^{2-} on the specimen surfaces [36,37]. Furthermore, we emphasized that based on the FT-IR spectra, the surfaces did not contain the sulphate group, SO_4^{2-}, as no peak was observed at the wavenumbers of 1072–1130 cm^{-1} [34,38]. The observed characteristics in FT-IR spectra imply the change in film composition from Cu_2O to Cu_2S between the sulphide contents of 3.2 mg/L and 32 mg/L. The findings also indicate that, besides the film composition, changes in the sulphide content of the test environment contributed to the other surface processes, such as the adsorption of sulphur-containing ions and, possibly, deposition.

Fig. 5a shows weight loss of the pre-oxidized specimens during the tests conducted utilizing various sulphide additions and further after the tests upon removal of the developed surface film. During the experiments, the most significant weight loss was detected for the specimens subjected to 3.2 mg/L sulphide, on average 0.34 g, followed by specimens subjected to 320 mg/L sulphide, 0.29 g. In the other two cases: in the absence of sulphides and at the sulphide content of 32 mg/L, weight loss of the specimens was much lower, 0.001 g and 0.003 g, respectively. Upon removal of the corrosion products, a clear increase in the extent of weight loss with raise the in sulphide content of the test environment was detected. Based on the observations from FT-IR measurements that Cu_2O (density 6.0 g/cm^3) was the main compound in the film up to the sulphide content of 3.2 mg/L, while Cu_2S (density 5.6 g/cm^3) was dominant in the film at higher sulphide contents, and the hypothesis about the uniformly distributed film on the specimen surfaces, weight losses could be converted into the film thickness (Fig. 5b). In the absence of sulphides in the simulated groundwater, the thickness of the film was 0.20 μm, whereas the film thickness of 0.62 μm was reached at the highest sulphide content.

Table 3 summarizes the chemistry of simulated groundwater with sulphide additions after the exposure of specimens for 9 months. When compared to the simulated groundwater without sulphide addition (7.9), the waters containing sulphide featured essentially higher pH

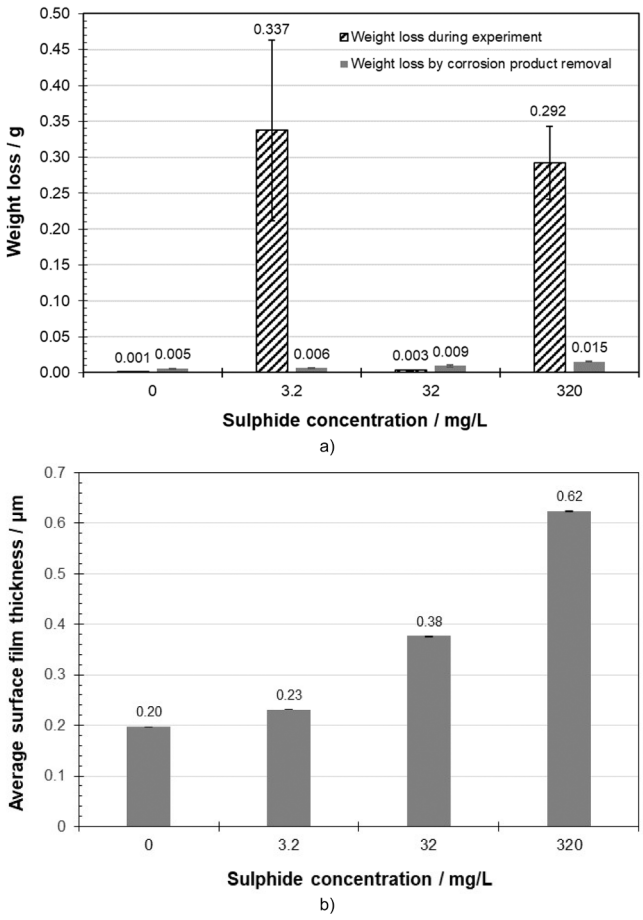

Fig. 5. a) Weight loss of the specimens during the test and by the corrosion product removal after the test. b) Average thickness of the corrosion product film deduced from weight loss of the specimens by corrosion product removal.

Table 3
Water chemistry after the exposure of specimens for 9 months. For comparison, the composition of the original simulated groundwater is given in Table 1.

		Sulphide addition			
Component	Unit	0 mg/L	3.2 mg/L	32 mg/L	320 mg/L
pH		7.9	8.5	8.7	10.0
Conductivity	mS/m	1640	1540	1660	1620
H_2S	mg/L	< 0.01	12	20	162
S^{2-}	mg/L	< 0.01	11	19	152
Cl^-	mg/L	5250	5400	5580	5410
Na^+	mg/L	2970	3260	3060	3530
SO_4^{2-}	mg/L	604	639	507	705
Ca^{2+}	mg/L	265	263	268	250
Mg^{2+}	mg/L	94	92	99	13
K^+	mg/L	52	53	53	52
Br^-	mg/L	43	41	44	42
HCO_3^-	mg/L	27	26	43	442
CO_3^{2-}	mg/L	0	3	5	62
CO_2 (tot)	mg/L	19	21	35	364
Alkalinity, pH 8.3	mmol/L	< 0.15	< 0.15	< 0.15	1.0
Alkalinity, pH 4.5	mmol/L	0.4	0.5	0.9	9.3
Sr^{2+}	mg/L	9.0	9.1	9.3	8.9
Si^{4+}	mg/L	6.9	6.7	5.1	0.3
B^{2+}	mg/L	1.9	1.6	2.2	3.9
F^-	mg/L	< 1.0	< 1.0	< 1.0	< 1.0
Cu, all	mg/L	0.4	< 0.01	< 0.01	< 0.01
Cu, soluble	mg/L	0.02	< 0.01	< 0.01	< 0.01

values, in the range from 8.5 (3.2 mg/L sulphide) to 10.0 (320 mg/L sulphide). The sulphide contents (H_2S, S^{2-}) revealed differences between the test environments: in the case of 3.2 mg/L sulphide addition, the

measured contents were slightly higher than the original (12 and 11 mg/L), while in the case of greater sulphide additions (32 mg/L and 320 mg/L), the measured contents after the exposures were lower than the original levels (20 and 19 mg/L; 162 and 152 mg/L). The two latter cases reflect the fact that some of the added sulphide is likely consumed, i.e., participated in the film formation. In the test environment with the highest sulphide content, some of the characteristics, e.g., concentrations of Mg^{2+}, HCO_3^- and Si^{4+} as well as alkalinity values, clearly deviated from the baseline, likely because of the higher pH than in other environments. The detected total and soluble copper (Cu^{2+}, Cu^{+}) levels of the waters after the exposures were low in all cases, yet the highest values were measured in the system with no sulphide addition. Especially in the case of the highest sulphide concentration, the changes in the groundwater chemistry are well in line with the observations from microstructural characterization, e.g., observations of magnesium and/or calcium by EDS and the presence of the adsorption band related to the carbonate group, CO_3^{2-}, in the FT-IR spectra. What the groundwater chemistry does not explain is the high weight loss during the test of specimens subjected to test environments with the sulphide contents of 3.2 mg/L and 320 mg/L. One could expect to see higher soluble Cu content of the groundwater in such cases.

In order to obtain improved understanding of the behaviour of specimens at the sulphide additions of 3.2 mg/L (surface film of Cu_2O) and 32 mg/L (surface film of Cu_2S), in-situ OCP and redox potential measurements were carried out. The results from OCP measurements showed that at the sulphide content of 3.2 mg/L, OCP values for the specimen were retained at a high level, at − 0.2 V vs. Ag/AgCl or above, through almost the entire exposure period. In earlier studies, such potential values have been associated with the formation of Cu_2O, e.g., [4,39,40]. Indeed, redox values of the electrolyte in the test were positive, in the range from 0.05 to 0.15 V vs. Ag/AgCl, for the majority of the exposure time, supporting the oxide film build-up. Conversely, in the test environment with the sulphide content of 32 mg/L, both the OCP value for the specimen and redox potential of the electrolyte were retained at much lower values, in the range from − 0.9 to − 0.85 V vs. Ag/AgCl and from − 0.5 to − 0.4 V vs. Ag/AgCl, respectively. This is well in agreement with the standard equilibrium potential of the Cu/Cu_2S couple, − 0.89 V. vs SHE [41] and what has been reported in the case of Cu_2S film development in literature, e.g., [6,11,41]. Therefore, we can conclude that the OCP results are in agreement with the results from FT-IR measurements.

The instantaneous CR for the copper specimens in the tests with 3.2 mg/L and 32 mg/L sulphide contents, respectively, was determined by the combination of in-situ Tafel and LPR measurements done intermittently during the exposure period. Overall, the derived CRs for the specimens at both sulphide contents (3.2 and 32 mg/L sulphide) were low, generally less than 5 μm/a, Fig. 6.7.8 However, differences in the CRs between the specimens exposed to the two sulphide contents were detected. CR of the specimen subjected to environment with 3.2 mg/L sulphide varied between 1 μm/a and 5 μm/a during the test, with the maximum values being detected at the initial stages and half-way of the exposure. In the case of specimen subjected to groundwater with 32 mg/L sulphide, the highest CR, 1.5 μm/a, was obtained at the beginning of the test, with the CR values decreasing steadily with time to the end value of 0.5 μm/a. Such low CR values are typical of the passive state [9,42,43]. These observations are well supported by the weight loss data, i.e., the overall lower weight loss of the specimens subjected to groundwater with 32 mg/L sulphide. One explanation is the uniform corrosion product film covering the surface, Fig. 3.

3.2. *Films developed on pre-oxidized and ground specimens at 32 mg/L of sulphide*

Fig. 9 shows SEM images of the corrosion product film morphology developed on ground specimens exposed to groundwater with 32 mg/L sulphide. For comparison, the corresponding images of pre-oxidized exposed specimens were presented in Fig. 3c. The greatest difference between the surface features is the essentially greater contribution of the original grinding grooves to the film morphology in the ground specimens, which is expected considering a smaller film thickness. However, it may be also possible that the morphology variations were affected by slight differences between polishing of individual specimens, as polishing was performed manually.

Fig. 9 shows the FT-IR spectra for the pre-oxidized and ground specimens exposed to simulated groundwater with the sulphide addition of 32 mg/L. In both specimens, the bands related to Cu_2S at 650 cm^{-1} and 2918 cm^{-1} could be detected, confirming the presence of Cu_2S. In particular, the band at 2918 cm^{-1} was pronounced in the case of ground specimen. Like in the case of pre-oxidized specimens above, adsorption bands related to the presence of air-containing species (H_2O, CO_2) and ionic species from the goundwater ($-CO_3^{2-}$) were detected in the spectra.

Fig. 10 shows the depth profiles for oxygen, sulphur and copper, obtained from GDOES, for the pre-oxidized specimen exposed to simulated groundwater with 32 mg/L sulphide addition. It is evident that the specimen surfaces contained both oxygen and sulphur (Fig. 10a), with copper being the dominating element only at the depth of 51 nm below the surface and beyond. A more detailed analysis (Fig. 10b) disclosed that the outermost areas of the specimen, down to the depth of about 20 nm, were essentially oxygen-rich, as the concentration of oxygen was higher than that of sulphur. With increase in the distance from the surface down to below 20 nm, sulphur became the dominating element

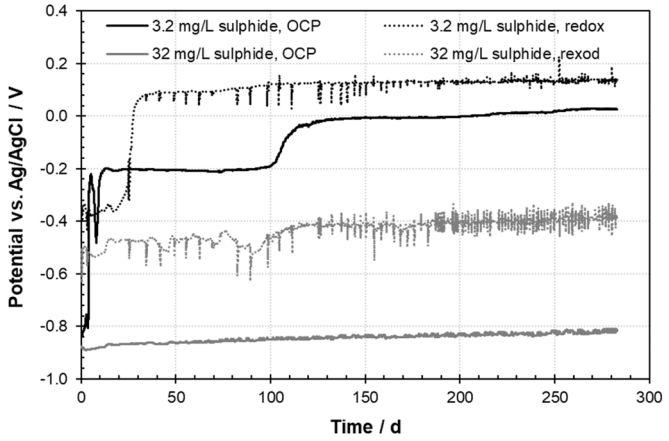

Fig. 6. Potential records from in-situ OCP and redox measurements during the exposure of pre-oxidized specimens to simulated groundwater with the two selected sulphide additions: 3.2 mg/L and 32 mg/L.

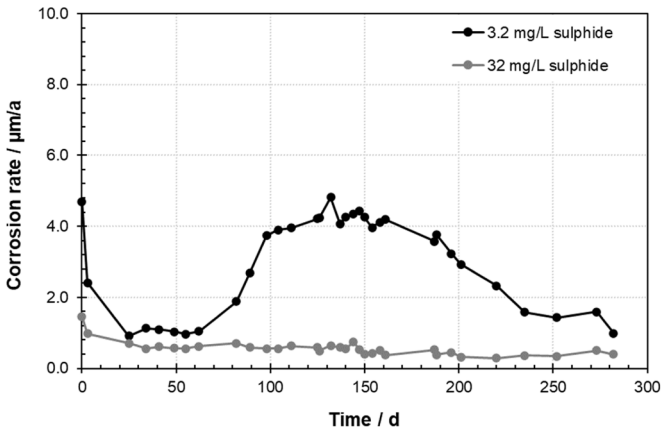

Fig. 7. Instantaneous CR defined based on in-situ LPR and Tafel measurements during the exposure of pre-oxidized specimens to simulated groundwater with the two selected sulphide additions: 3.2 mg/L and 32 mg/L.

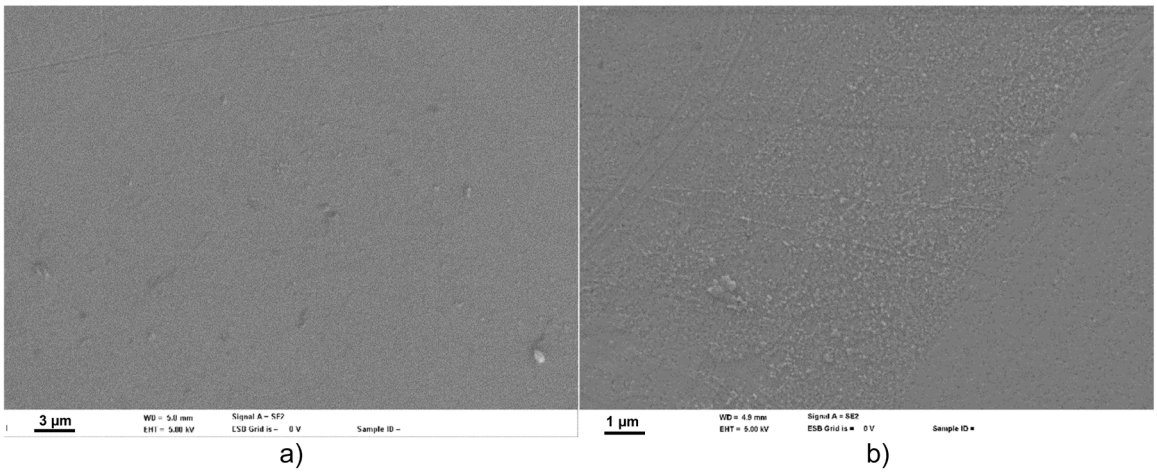

Fig. 8. SEM images taken at various magnifications, showing the morphology of ground specimens exposed to simulated groundwater with the sulphide addition of 32 mg/L.

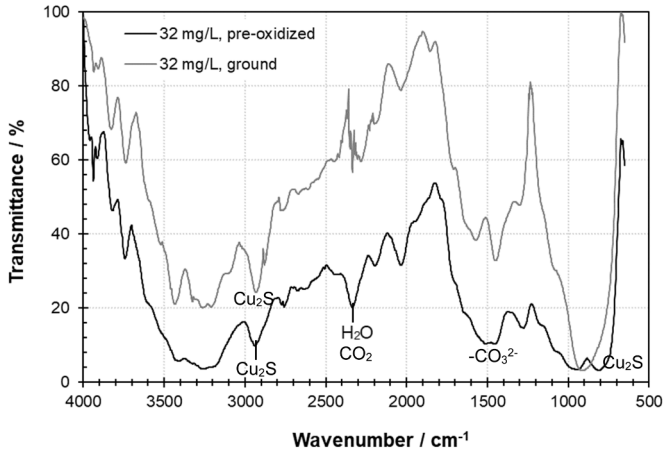

Fig. 9. FT-IR spectra for pre-oxidized and ground specimens exposed to simulated groundwater with the sulphide addition of 32 mg/L.

in the specimen. This suggests that a sulphur-rich layer exists beneath the oxygen-rich layer, consistent with our recent results obtained by time-of-flight secondary ion mass spectroscopy [16]. The maximum mass concentration of both elements, 33% in the case of oxygen and 41% in the case of sulphur, was detected at the depth of 43 nm. However, the surface region was sulphur-rich down to the depth of 100 nm. It is worth mentioning that copper contributed to GDOES data only at the depth of 44 nm and below, indicating that the outermost oxygen-rich areas were likely related to the deposition of oxygen-bearing species (such as carbonate compounds, as indicated by the carbonate group in FT-IR spectrum) on the specimen surface rather than the presence of copper-oxygen compounds. Nevertheless, based on these observations it is also evident that a corrosion product film composing of sulphur- and oxygen-compounds of copper covered the metal. Altogether, copper corresponded to 95 wt.-% of the analyzed material at the depth of 290 nm and 98 wt.-% of the material at the depth of 800 nm.

In the case of specimen with the ground surface finish exposed to simulated groundwater with 32 mg/L sulphide addition, GDOES investigations revealed that copper corresponded to the majority of the material mass (mass concentration) already at the surface (Fig. 11). However, the surface was evidently enriched in sulphur and oxygen, at maximum 25% and 12%, respectively, suggesting the presence of sulphur- and oxygen-containing compounds of copper, i.e., the surface

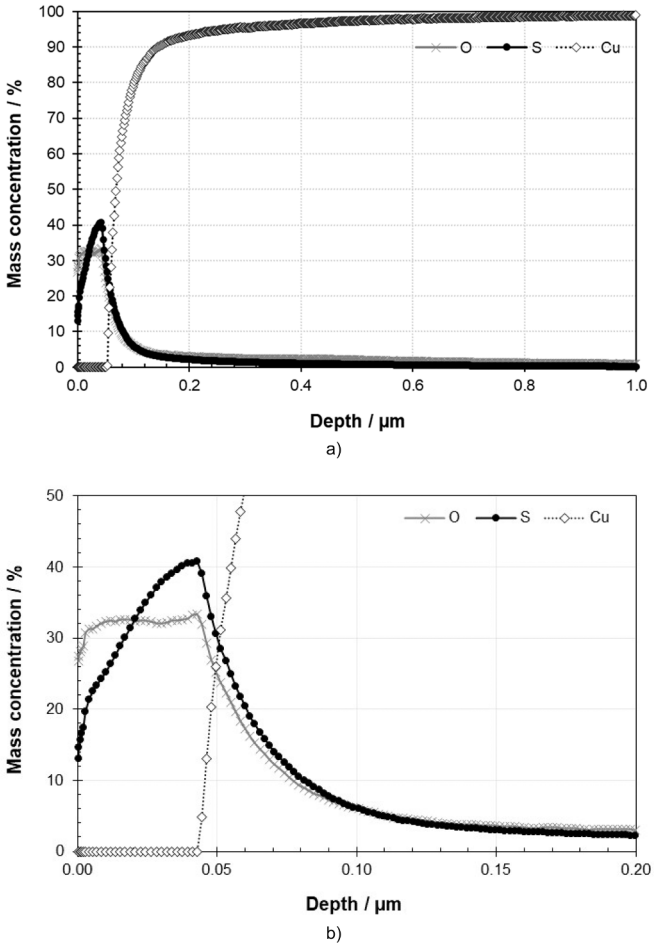

Fig. 10. Elemental depth profiles of oxygen, sulphur and copper for pre-oxidized specimen exposed to simulated groundwater with 32 mg/L sulphide addition. a) Profile down to the depth of 1.0 µm. b) Zoomed profile down to the depth of 0.2 µm.

film. The concentration of both sulphur and oxygen decreased with increase in depth. Sulphur was the primary element in the surface film down to the depth of 43 nm, with oxygen dominating at greater depths yet at very low contents. At the depth of 40 nm already 95% of the GDOES signal originated from copper. At the depth of 210 nm below the

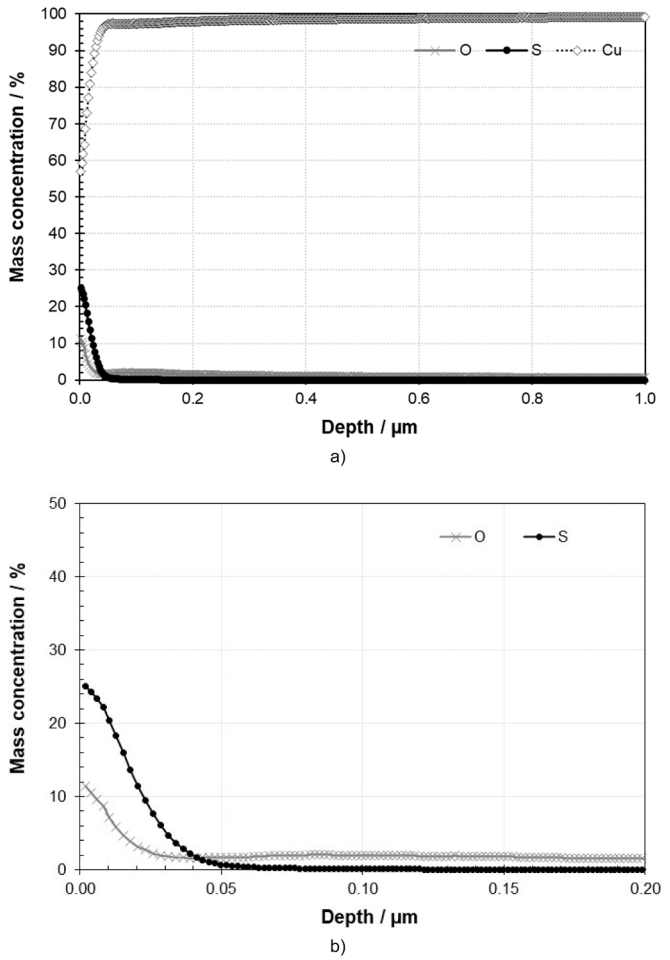

Fig. 11. Elemental depth profiles of oxygen, sulphur and copper for ground specimen exposed to simulated groundwater with 32 mg/L sulphide addition. a) Profile down to the depth of 1.0 µm. b) Zoomed profile down to the depth of 0.2 µm.

surface, 98% of the material corresponded to copper. These results indicated that the surface film was clearly thinner on ground copper specimen than on the pre-oxidized copper specimen.

Fig. 12a shows weight loss of the pre-oxidized and ground specimens during the experiment and further upon the corrosion product removal. Two main findings can be made. First, weight losses during the experiment were relatively higher in the case of pre-oxidized copper specimens (on average 0.003 g) than for ground specimens (0.001 g), hence the surface film that developed on ground specimens was likely more protective against corrosion than the one on pre-oxidized specimens. Second, the weight losses by corrosion product removal were greater in ground specimens (0.012 g) than in pre-oxidized specimens (0.008 g), indicating the surface film that developed during the exposure was thicker and/or denser in ground specimens. Assuming a uniform coverage of the surfaces by the film, weight losses by corrosion product removal turned into the film thickness of 0.38 µm in pre-oxidized specimens and 0.49 µm in ground specimens (Fig. 12b). These film thicknesses are evidently of the same magnitude as revealed above by the GDOES measurements, considering the definition of boundary between the corrosion product and the substate where the metal content reaches the magnitude of 95–98%. It will be later shown that the definition of the film thickness is not unambiguous because of the deposition of compounds, e.g., carbonates, surface roughness of the metal surface prior to the experiment, and the local variations in the corrosion product morphology that imply some scatter in the thickness between local areas.

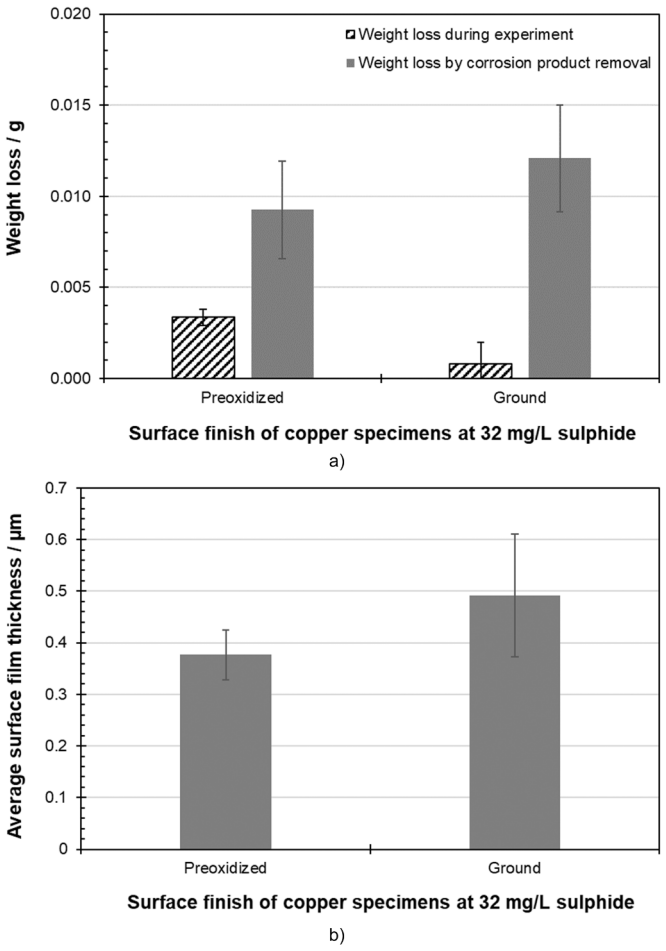

Fig. 12. a) Weight loss of the specimens during the test and by the corrosion product removal after the test. b) Average thickness of the corrosion product film deduced from weight loss of the specimens by corrosion product removal.

4. Discussion

4.1. Film structure and composition

The obtained results clearly show that in pre-oxidized copper specimens exposed to simulated groundwater with sulphide, the composition of the surface film is dependent on the sulphide content of the environment. At the sulphide contents of 3.2 mg/L and below, cupric oxide, Cu_2O, was the primary compound detected in the surface film on the specimens, the observation which is supported by electrochemical results. Increasing the sulphide content of the groundwater to 32 mg/L and beyond changed the film composition, introducing mainly Cu_2S. This observation was verified by FT-IR analyses and electrochemical data, in particular the OCP measurements. The chemical analyses of the groundwaters after the exposure of specimens for 9 months similarly revealed a change in some key chemical characteristics when increasing the sulphide content to 32 mg/L and beyond, especially the decrease in sulphide content of the solution and the increase in the solution pH. These are likely essentially linked with the same reaction, i.e., the build-up of the Cu_2S film according to [12,15]:

$$Cu_2O + SH^- \rightarrow Cu_2S + OH^- \quad (4)$$

in which the following cathodic reduction of Cu_2O [12]:

$$Cu_2O + 2e^- + H_2O \rightarrow 2\,Cu + 2OH^- \quad (5)$$

is coupled to the anodic formation of Cu_2S:

$$2Cu + SH^- \rightarrow Cu_2S + H^+ + 2e^- \quad (6)$$

It can be seen that Reactions 4 and 5 release hydroxide ions that contribute to the increase in solution pH. In contrast to these, Reaction 6 generates protons that lower the solution pH.

In the analysis of the obtained results, we have to bear in mind the capabilities of used research methods. Electrochemical methods are continuum methods in the sense that they provide from the entire exposed surface following mixed potential theory, and LPR and Tafel analyses yield instantaneous corrosion rates. FT-IR method is based on the reflection of light, therefore only the external areas of (opaque) specimens contribute to the measured signal. Areas of uniform surface structure were selected for the investigation, therefore these sections compose of Cu_2S. However, what lies underneath, can be best revealed by GDEOS method. The GDOES data originates from area of approximately 2.5 mm in diameter, hence the obtained response likely originates from several grains (the grain structure is shown in ref. [16]) in lateral dimension, but likely from one grain only in the depth direction. As revealed by GDOES examinations, both pre-oxidized and ground specimens contained oxygen in the surface film along with sulphur. Our interpretation is that the surface film is actually the admixture of Cu_2S and Cu_2O, meaning that both compounds are included in the surface film. At greater depths, i.e., underneath the mixture of Cu_2S and Cu_2O, minor amounts of oxygen were detected (1–5%). Therefore, we cannot completely exclude the idea that Cu_2O acts as a bridge layer between Cu_2S and metallic Cu [14]. We acknowledge that thermodynamics predicts the complete conversion of Cu_2O into Cu_2S, and the fact that the experiments in this work may have been kinetically too short for a complete conversion.

Both Cu_2O and Cu_2S are *p*-type semiconductors [8,9,44,45]. A theoretical approach implies that semi-conducting (passive) films comprise of two layers: a point-defective barrier layer that contains cation vacancies, oxygen/sulphur vacancies and interstitials, and grows directly into the metal, as well as a porous precipitated outer layer. The barrier layer growth occurs by the generation of oxygen (or sulphur) vacancies at the metal/barrier layer interface and their annihilation at the barrier layer/solution interface. Simultaneously, cation vacancies are formed at the film/solution interface and move to the metal/film interface, where they are annihilated [46,47]. Thus, the barrier film acts as a semi-permeable membrane, enabling the travel of oxygen or sulphide anions along oxygen/sulphur vacancies to the metal/barrier layer interface and that of metal cations towards the barrier layer/solution interface. The described film build-up mechanism could explain the co-existence of oxygen and sulphur in the surface films that are evolved on the specimens in simulated groundwater with sulphide, Figs. 10 and 11. However, it is evident that more research is needed in this area, to prove the mechanism of conversion of Cu_2O into Cu_2S. More importantly, further work is needed to explore the ingress of reactive species, such as oxygen, sulphur, and hydrogen, into the copper substrate and the possible consequences, e.g., embrittlement [16].

An interesting question is the definition of the film thickness, i.e., where it starts and where it ends. When considering the outermost areas of the surface, particularly the pre-oxidized specimen exposed to groundwater with 32 mg/L sulphide contained deposit that was clearly precipitated from groundwater because of the changes in water chemistry ($MgCO_3$ and/or $CaCO_3$). This adds thickness of the surface film on the specimens, yet it has developed by a completely different mechanism than the actual corrosion product film. As copper is an inherent element in the corrosion product film, we define the solution/film interface at the first depth point with signal from Cu. In the other extreme, the concentration profiles for both oxygen and sulphur are quite smooth, likely because of several overlapping reasons: surface roughness of the film, possible roughness in the film/substrate interface across the grains, and ingress of corrosive elements into copper [16]. However, small amounts (1–5%) of oxygen were detected at depths where the sulphur signal was attenuated. Therefore, the most reasonable way of defining the film/substrate interface is the depth where oxygen concentration exceeds that of sulphur. Following such definitions, we end up in the approximate film thicknesses of 60 nm and 40 nm for pre-oxidized and ground specimens, respectively. This indicates that the pre-oxidation of copper specimens adds film thickness. An interesting reference data for the GDOES results is the weight loss data, more specifically the weight loss by the removal of corrosion products. This approach gave almost ten times higher film thickness values as compared to GDOES analysis. However, we must remember that weight loss data is generated across the entire exposed surface and includes not only the contribution by chemical deposits formed during the exposure but also the influence of nodular growth of the film. Analysis spots for GDOES measurements, like for FT-IR investigations, selected among smooth areas.

4.2. Used characterization methods

FEG-SEM is a powerful universal research tool enabling insights into the surface morphology of plane specimens [48]. The good electrical conductivity of the specimen is of importance, otherwise the specimen will be charged. In this work we did not observe any indication of charging during FEG-SEM investigations of specimens from corrosion experiments, therefore the developed corrosion product films were essentially conductive. However, further analyses, related either to thickness or composition of the corrosion product films, are limited by the spatial resolution of the techniques. For example, the interaction volume of EDS analyses, representing the region of X-ray excitation within the specimen, is typically of the magnitude of micrometers. This applies also to the depth resolution: majority of data originates from the depth greater than a micrometer, therefore the method may provide *indication* of which elements exists in the surface, but the exact values are meaningless. The corrosion product films included in this research were too thin and structurally heterogeneous to be reproducibly studied in cross-section. Applying focussed ion beam (FIB) milling to the specimens might have helped to examine the cross-sectional specimens, and this is one interesting option for the future research.

The thickness of developed corrosion product films, of the magnitude of from some tens to some hundreds of nanometers, was the factor determining the selection of compositional analysis techniques. The two main methods that were used were FT-IR and GDOES, with the former being at its best in detecting functional groups in the surface and the latter in depth profiling of selected elements. The results obtained by the two methods were well in agreement with each other, although GDOES analyses were performed only for few specimens. For example, FT-IR analyses for the pre-oxidized specimens subjected to simulated groundwater with 32 mg/L sulphide revealed the presence of main compounds and functional groups, such as Cu_2S and -CO_3^{2-}, while GDOES analyses for the same specimen revealed the presence of oxygen at the near-surface areas followed by a layer containing sulphur, copper and some oxygen. We have previously [16] analysed the parallel specimen using TOF-SIMS method, with very similar results: the outermost areas were essentially oxygen- and sulphur-rich. Nevertheless, TOF-SIMS method was also capable of revealing the depth distribution of Cl^-, OH^- and H^-, with Cl^- level within corrosion product film being constant and essentially higher than in the bulk metal, OH^- following the same trend as sulphur (maximum at the depth of approximately 25 nm and with a slow decay down to about 120 nm), and H^- showing a steadily decreasing trend upon moving from the surface to the substrate. DGOES revealed sulphur penetration down to the depth of 100 nm, while TOF-SIMS showed the presence of sulphur down to the depth of 147 nm [16]. Keeping in mind the heterogeneous nature of the corrosion product film, the methods gave surprisingly equal results. We also highlight that the water chemistry analyses that were done after the exposures revealed trends that could be linked with the observed corrosion product film development.

The use of complementary methods, like electrochemical methods and weight loss measurements, was essential to verify our observations

from specimen characterization. In particular, electrochemical methods are surface sensitive, hence they introduce the averaged response from electrochemical reactions at conducting surfaces. Also these results seamlessly supported the findings from specimen characterization, e.g., OCP measurements were in the favour of the development of Cu_2S pre-oxidized specimens subjected to simulated groundwater with 32 mg/L sulphide. The purpose of weight loss measurements was to provide general information about the behaviour of specimens during the exposures and, in particular, the corrosion product film thicknesses. Weight losses during the exposures indicated significant material losses during the exposures at the sulphide contents of 3.2 mg/L and 320 mg/L, but we could not directly correlate these observations with e.g., and water chemistry analyses. We expect that the proved heterogeneous nature of the corrosion product films may have contributed to the results, e.g., gentle cleaning of the exposed specimens before weighing may have removed some of the loose grains in the film. However, weight losses upon the corrosion product removal gave relatively consistent results with those from microstructural characterization, keeping in mind their completely different nature: values from weight loss measurements give the average thickness of the film in the specimen using the selected cleaning procedure, whereas DGOES analyses represent one local (uniform) area in the specimen.

We acknowledge that there are also some microstructural features that cannot be disclosed by the combination of methods we applied. For example, based on our results, we know that sulphur and oxygen coexist in the corrosion product film, but we don't know exactly how the compounds, Cu_2S and likely Cu_2O, are distributed in the film growth direction. This is one area we plan to put more effort in the future via transmission electron microscopy (TEM) investigations. To conclude, it is evident that in the research of corrosion product films, the most fruitful approach is to employ many characterization methods in parallel that rely on diverse operation principles. We also need to accept that not all techniques work in all specimens. For example, we tried to apply Raman spectroscopy for the characterization of our specimens, but the corrosion product films were essentially too thin for the depth resolution of the method.

5. Conclusions

This research has focussed on characterization of the surface films that develop on copper in anoxic simulated groundwater as such and with three different sulphide additions. Most of the specimens exposed to the test environments were in pre-oxidized condition, yet some tests involved also freshly ground copper specimens, aiming to clarify the role of pre-existing oxide film on the film chemistry. The following conclusion can be drawn based on the obtained results:

Composition of the surface film is dependent on the sulphide content of the test environment. In the simulated groundwater as such and at the sulphide content of 3.2 mg/L, cupric oxide, Cu_2O, was the primary compound detected in the surface film. Increasing the sulphide content of the groundwater to 32 mg/L and beyond changed the film composition, introducing Cu_2S.

The surface films that developed on copper were continuous and covered the specimens fully, yet they were structurally heterogeneous. Nodular film growth was observed on top of the thinner section of the film in many cases. Weight loss measurements disclosed that the film thickness increased generally with increase in sulphide content, yet such finding may be influenced by other parallel phenomena, such as build-up of chemical deposits on the specimen surface leading to water chemistry changes.

GDOES analyses disclosed that sulphur and oxygen coexist in the surface film all through the film thickness, yet the outermost areas are essentially rich in sulphur. This is consistent with FT-IR analyses that revealed Cu_2S, hence it is likely that Cu_2S and Cu_2O coexist in the film. Based on the obtained results, it seems that the pre-existing oxide film (formed by pre-oxidation treatment or naturally in air) promotes the development of the corrosion product film and penetration of sulphur to film/metal interface, as reflected by the greater thickness of sulphur-containing layer. However, it is evident that more research is needed to demonstrate the mechanism of Cu_2S build-up on Cu_2O.

In the research of corrosion product films, the most fruitful approach is to employ many characterization methods, relying on diverse operation principles, in parallel. The film thickness becomes of importance particularly when characterizing the specimens ex-situ and determines the selection of applicable methods.

CRediT authorship contribution statement

V. Ratia-Hanby: Investigation, Methodology, Writing. **E. Isotahdon:** Funding acquisition, Project administration, Resources, Methodology, Writing. **X. Yue:** Investigation, Writing. **P. Malmberg:** Investigation. **Writing. C. Leygraf:** Funding acquisition, Supervision. **Writing. J. Pan:** Funding acquisition, Project administration, Resources, Methodology, Supervision, Writing. **E. Huttunen-Saarivirta:** Funding acquisition, Supervision, Methodology, Writing.

Declaration of Competing Interest

The authors declare the following financial interests/personal relationships which may be considered as potential competing interests. Elisa Isotahdon reports financial support was provided by NKS.

Data Availability

Data will be made available on request.

Acknowledgements

The COCOS project has been funded by Nordic Nuclear Safety Research NKS, via contracts AFT/NKS-R(19-21)127, and by two affiliated organizations: VTT Technical Research Centre of Finland Ltd and KTH Royal Institute of Technology in Sweden. The financial support is gratefully acknowledged. Additionally, the authors wish to thank the following colleagues that have helped in the lab work: Mr. Tuomo Kinnunen and Mrs. Taru Lehtikuusi (corrosion tests), Mr. Harri Joki (FT-IR measurements), and Mrs. Mervi Somervuori (SEM).

References

[1] F. King, C. Lilja, K. Pedersen, P. Pitkänen, An update of the state of the art report on the corrosion of copper under expected conditions in a deep geologic repository. 31, 2012, 180.
[2] T. Salonen, T. Lamminmäki, F. King, B. Pastina, Status report of the Finnish spent fuel geologic repository programme and ongoing corrosion studies, Mater. Corros. 72 (2021) 14–24.
[3] D.D. Macdonald, S. Sharifi-Asl, Is copper immune to corrosion when in contact with water and aqueous solutions? Strål säkerhets myndigheten report 2011: 09.
[4] E. Huttunen-Saarivirta, P. Rajala, M. Bomberg, L. Carpén, EIS study on aerobic corrosion of copper in ground water: influence of micro-organisms, Electrochim. Acta 240 (2017) 163–174.
[5] Z. Chen, D.W. Qin, Shoesmith, Kinetics of corrosion film growth on copper in neutral chloride solutions containing small concentrations of sulphide, J. Electrochem. Soc. 157 (2010) C338–C345.
[6] T. Martino, R. Partovi-Nia, J. Chen, Z. Qin, D.W. Shoesmith, Mechanisms of film growth on copper in aqueous solutions containing sulphide and chloride under voltametric conditions, Electrochim. Acta 127 (2014) 439–447.
[7] J. Chen, Z. Qin, D.W. Shoesmith, Long-term corrosion of copper in a dilute anaerobic sulfide solution, Electrochim. Acta 56 (2011) 7854–7861.
[8] D. Kong, A. Xu, C. Dong, F. Mao, K. Xiao, X. Li, D.D. Macdonald, Electrochemical investigation and ab initio computation of passive film properties on copper in anaerobic sulphide solutions, Corros. Sci. 116 (2017) 34–43.
[9] F. Mao, C. Dong, S. Sharifi-Asl, P. Lu, D.D. Macdonald, Passivity breakdown on copper: influence of chloride ion, Electrochim. Acta 144 (2014) 391–399.
[10] M. Marja-aho, P. Rajala, E. Huttunen-Saarivirta, A. Legat, A. Kranjc, T. Kosec, L. Carpén, Copper corrosion monitoring by electrical resistance probes in anoxic groundwater in the presence and absence of sulfate reducing bacteria, Sens. Actuators A 274 (2018) 252–261.

[11] E. Huttunen-Saarivirta, P. Rajala, L. Carpén, Corrosion behaviour of copper under biotic and abiotic conditions in anoxic ground water: electrochemical study, Electrochim. Acta 203 (2016) 350–365.
[12] J.M. Smith, J.C. Wren, M. Odziemkowski, D.W. Shoesmith, The electrochemical response of preoxidized copper in aqueous sulfide solutions, J. Electrochem. Soc. 154 (2007). C431-C438.
[13] A. Forsström, R. Becker, H. Hänninen, Y. Yagodzinskyy, M. Heikkilä, Sulphide-induced stress corrosion cracking and hydrogen absorption of copper in deoxygenated water at 90°C, Mater. Corros. 72 (2021) 317–332.
[14] J.H. Stenlid, E.C. dos Santos, A.J. Johansson, L.G.M. Pettersson, Properties of interfaces between copper and copper sulphide/oxide films, Corros. Sci. 183 (2021), 109313.
[15] H.M. Hollmark, P.G. Keech, J.R. Vegelius, L. Werme, L.C. Duda, X-ray absorption spectroscopy of electrochemically oxidized Cu exposed to Na_2S, Corros. Sci. 54 (2012) 85–89.
[16] X. Yue, P. Malmberg, E. Isotahdon, V. Ratia-Hanby, E. Huttunen-Saarivirta, C. Leygraf, J. Pan, Penetration of corrosive species into copper exposed to simulated O_2-free groundwater by time-of-flight secondary ion mass spectrometry (ToF-SIMS), Corros. Sci. 210 (2023), 110833.
[17] U. Vuorinen, K. Ollila, M. Snellman, Groundwater chemistry at Olkiluoto -Saline and brackish groundwater –Recipe for saline reference water. Posiva working report 1997–25.
[18] D.A. Jones, Principles and Prevention of Corrosion, Macmillan Publishing Company, Singapore, 1992.
[19] ASTM G1–03. Standard practice for preparing, cleaning, and evaluating corrosion test specimens.
[20] G.W. Poling, Infrared reflection studies of the oxidation of copper and iron, J. Electrochem. Soc. 116 (1969) 958–963.
[21] D. Persson, C. Leygraf, In situ infrared reflection absorption spectroscopy for studies of atmospheric corrosion, J. Electrochem. Soc. 140 (1993) 1256–1260.
[22] A. Labberti, M. Desrro, S. Bianco, M. Quaglio, A. Chiodoni, C.F. Pirri, C. Gerbaldi, Facile fabrication of cuprous oxide nanocomposite anode films for flexible Li-ion batteries via thermal oxidation, Electrochim. Acta 86 (2012) 323–329.
[23] M. Justin Paul, R. Suresh, R. Marnadu, V. Balasubramani, Amelioration of rectification properties of CuO nanostructures using surface modification, Opt. Mater. 131 (2022), 112732.
[24] V. Navakoteswara Rao, P. Ravi, M. Sathish, M. Sakar, B.Lyong Yang, J.-M. Yang, M. Mamatha Kumari, M.V. Shankar, Titanate quantum dots-sensitized Cu_2S nanocomposites for superficial H_2 production via photocatalytic water splitting, Int. J. Hydrog. Energy 47 (2022) 40379–40390.
[25] B. Chu, X. Ou, L. Wei, H. Liu, K. Chen, L. Meng, M. Fan, B. Li, L. Dong, Insight into the effect of oxygen vacancies and OH groups on anatase TiO_2 for CO oxidation: a combined FT-IR and density functional theory study, Mol. Catal. 511 (2021), 111755.
[26] B. Shi, F. Chu, X. Wang, L. Wei, M. Teng, B. Fan, L. Li, L. Dong, Dong, Mn-modified CuO, $CuFe_2O_4$, and γ-Fe_2O_3 three-phase strong synergistic coexistence catalyst system for NO reduction by CO with a wider active window, ACS Appl. Mater. Interfaces 10 (2018) 40509–40522.
[27] A. Sharma, A. Yadav, S.K. Sharma, R.K. Sharma, Laser induced morphology change in copper sulphide nanoparticles, Colloids Surf. A 565 (2019) 172–179.
[28] O. Mabayoje, M. Seredych, T.J. Bandosz, Cobalt (hydr)oxide/graphite oxide composites: Importance of surface chemical heterogeneity for reactive adsorption of hydrogen sulfide, J. Colloid Interface Sci. 378 (2012) 1–9.
[29] M. El-Mazaawi, A.N. Finken, A.B. Nair, V.H. Grassian, Adsorption and photocatalytic oxidation of acetone on TiO_2: an in situ transmission FT-IR study, J. Catal. 191 (2000) 138–146.
[30] C.A. Melendres, G.A. Bowmaker, J.M. Leger, B. Beden, In-situ syncrothron far infrared spectroscopy of surface films on a copper electrode in aqueous solutions. J. Electroanal. Chem. 449 (1998) 215–218.
[31] H. Yang, J. Ouyang, A. Tang, Y. Xiao, X. Li, X. Dong, Y. Yu, Electrochemical synthesis and photocatalytic property of cuprous oxide nanoparticles, Mater. Res. Bull. 41 (2006) 1310–1318.
[32] S.G. Dixit, A.R. Mahadeshwar, S.K. Haram, Some aspects of the role of surfactants in the formation of nanoparticles, Colloids Surf. A 133 (1998) 69–75.
[33] S. Fakhravar, M. Farhadian, S. Tangestaninejad, Excellent performance of a novel dual Z-scheme $Cu_2S/Ag_2S/BiVO_4$ heterostructure in metronidazole degradation in batch and continuous systems: immobilization of catalytic particles on a-Al_2O_3 fiber, Appl. Surf. Sci. 505 (2020), 144599.
[34] S. Yadav, K. Shrivas, P.K. Bajpai, Role of precursors in controlling the size, shape and morphology in the synthesis of copper sulfide nanoparticles and their application for fluorescence detection, J. Alloy. Compd. 772 (2019) 579–592.
[35] E. Breysse, F. Fajula, A. Finiels, G. Frémy, J. Lamotte, F. Maugé, J.-C. Lavalley, C. Moreau, Kinetic and FT-IR study for the mechanism of addition of hydrogen sulfide to methyl acrylate over solid basic catalysts, J. Mol. Catal. 198 (2003) 185–194.
[36] X. Bi, N. Yao, X. Meng, M. Gou, P. Zhao, $MnCO_3$-catalyzed transesterification of alcohols with dimethyl carbonate under mild conditions, Catal. Lett. 151 (2021) 454–462.
[37] A. Kaflak, A. Ślósarczyk, W. Kolodziejski, A comparative study of carbonate bands from nanocrystalline carbonated hydroxyapatites using FT-IR spectroscopy in the transmission and photoacoustic modes, J. Mol. Struct. 997 (2011) 7–14.
[38] X. Jinxia, T. Qiping, M. Youjing, Corrosion protection of steel by Mg-Al layered double hydroxides in simulated concrete pore solution: Effect of SO_4^{2-}, Corrosion Science 163 (2020) 108223.
[39] E. Huttunen-Saarivirta, P. Rajala, M. Bomberg, L. Carpén, Corrosion of copper in oxygen-deficient groundwater with and without deep bedrock micro-organisms: characterization of microbial communities and surface processes, Appl. Surf. Sci. 396 (2017) 1044–1057.
[40] T. Kosec, Z. Qin, J. Chen, A. Legat, D.W. Shoesmith, Copper corrosion in bentonite/saline groundwater solution: effects of solution and bentonite chemistry, Corros. Sci. 90 (2015) 248–258.
[41] J. Smith, Z. Qin, F. King, L. Werme, D.W. Shoesmith, Sulfide film formation on copper under electrochemical and natural corrosion conditions, CORROSION 63 (2007) 135–144.
[42] D. Kong, C.-F. Dong, K. Xiao, X.-G. Li, Effect of temperature on copper corrosion in high-level nuclear waste environment, Trans. Nonferrous Met. Soc. China 27 (2017) 1431–1438.
[43] E. Huttunen-Saarivirta, E. Isotahdon, M. Lindgren, A. Mardoukhi, P. Mocnik, T. Kosec, J.B. Jorcin, S. Hägg Mameng, Y. El Ouazari, L. Wegrelius, Corrosion of stainless steels S31603, S31655, and S32101 in sulfuric acid solutions: effects of concentration, chlorides and temperature, CORROSION 78 (10) (2022) 943–962.
[44] A. Xu, C. Dong, X. Wei, X. Li, D.D. Macdonald, DFT and photoelectrochemical studies of point defects in passive films on copper, J. Electroanal. Chem. 834 (2019) 216–222.
[45] A. Xu, C. Dong, X. Wei, F. Mao, X. Li, D.D. Macdonald, Ab initio calculation and electrochemical verification of a passivated surface on copper with defects in 0.1 M NaOH, Electrochem. Commun. 68 (2016) 62–66.
[46] D.D. Macdonald, The Point Defect Model for the passive state, J. Electrochem. Soc. 139 (1992) 3434–3449.
[47] D.D. Macdonald, The history of the Point Defect Model for the passive state: a brief review of film growth aspects, Electrochim. Acta 56 (2011) 1761–1772.
[48] E. McCafferty, New York, USA. Introduction to Corrosion Science, Springer,, 2010.